The Hat Creek Radio Observatory
ATA Beamformer efficiency

Wael Farah

Pranav Premnath

SETI Institute
189 Bernardo Ave, Suite 200
Mountain View, CA 94043
wfarah@seti.org

February 10, 2022

1 Introduction

Beamforming, in the receiving paradigm, is a process of combining multiple elements to maximize the sensitivity towards a specific direction. Given a model of the geographic distribution of the telescope stations, and an empirical measurement of the instrumental delays due to the different cable/fiber delays from each element to the digitizers, the necessary delays for every station can computed and applied on every voltage stream. Voltages from each station can then be added to produce a phased-array beam at the direction of interest.

A simple, but yet powerful diagnostic of the performance of the beamformer is to measure the signal-to-noise improvement as a function of incremental addition of antennas added to the coherent sum. The curve ideally should follow a linear trend. This memo describes an experiment performed on a geostationary satellite that allowed such a measurement.

2 Experiment

To measure the beamformer efficiency, one would like to utilise a bright source to reduce perturbations in the S/N measurements. The source of choice was `GOES-16`, a geostationary satellite used for various weather and atmospheric experiments. The satellite is located along the 75th meridian west, and has coordinates of Az, El = $(121.945, 23.607)$ at the position of the ATA. The GOES-16 Rebroadcast (GRB, see this) downlink from the satellite is centered at 1686.6 MHz, and spans around 10 MHz of bandwidth.

On Wednesday January 12th 2022, 20 ATA antennas, including 19 fitted with new Antonio feeds, were pointed at the `GOES-16` satellite. Tuning B was used for the experiment, and the focus feeds were centred at the frequency of the source transmitter. Twenty seconds of baseband voltage data with all 20 antennas, using the newly deployed RFSoC boards, were recorded to the NVMe sticks. Antenna 1e (new feed) was later excluded from the data given a failure mode that had occurred earlier that week which caused the cryocooler to switch off and the feed to warm up.

For this experiment, the RFSoC delay engine was loaded with the latest instrumental delay solutions obtained on a bright wideband astronomical source, and was commanded to delay the antennas, with respect to reference antenna 1c, given the coordinates of the satellite. As phase calibration was needed before performing antenna summing, a previous recording was performed on the satellite, and the calibration procedure is described in the following section.

2.1 Calibration

Calibrating a beamformer is an inherently difficult task. One has to accurately measure residual delays and phase offsets that are present due to various cable length variations and electronic circuitry, and apply those solutions for subsequent recordings. In order to do that, following typical radio astronomy procedures for

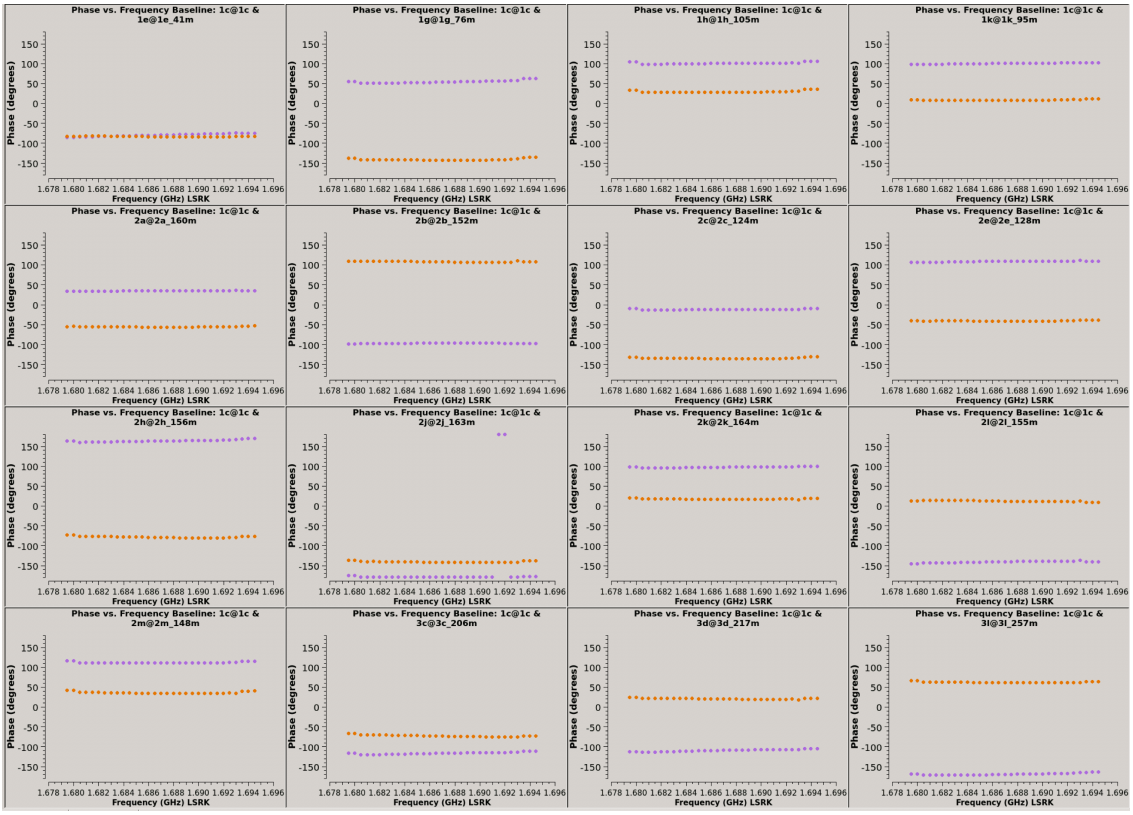

Figure 1: The cross-correlation data products obtained by the offline correlator, while pointed at the source of interest, `GOES-16`. Purple represents the X-polarization, whereas orange represents the Y-polarization. Each subplot represents the cross-correlation of antenna `1c` against the others. Phase offset, that will be calibrated for, are observed.

wide-band systems such as the ATA, a correlator is deployed to perform these measurements. The correlator's data output is a set of cross-antenna multiplication data products. Fig. 1 shows the phase vs frequency plots for an observation of `GOES-16`, zoomed into the 10MHz around the center center frequency of the transmitter. The plot was produced with CASA, the Common Astronomy Software Applications package, a go-to data processing software used to reduce radio astronomy data. In the plot, purple represents the X-polarization, whereas orange represents the Y-polarization. Every subplot represents the correlation product of all antennas against our reference antenna `1c`. Residual delays would manifest as linear trends in the phase vs frequency plots, a phenomenon not seen in the plot. This is due to the fact that the delay engine was utilising a correct delay solution that was obtained on a previous observation of an astronomical source. Phase offset residuals, however, do exist. The already existent phase solution does not account for the phase offset within the frequency band that `GOES-16` transmitter operates at, for the natural reason that this band would have been excised in the prior astronomical calibrator observation. `GOES-16` is bright enough that it might have been coupled through the sidelobes of the beams in that prior recording. Hence, a phase solution for every antenna-polarization is determined using the data of Fig. 1.

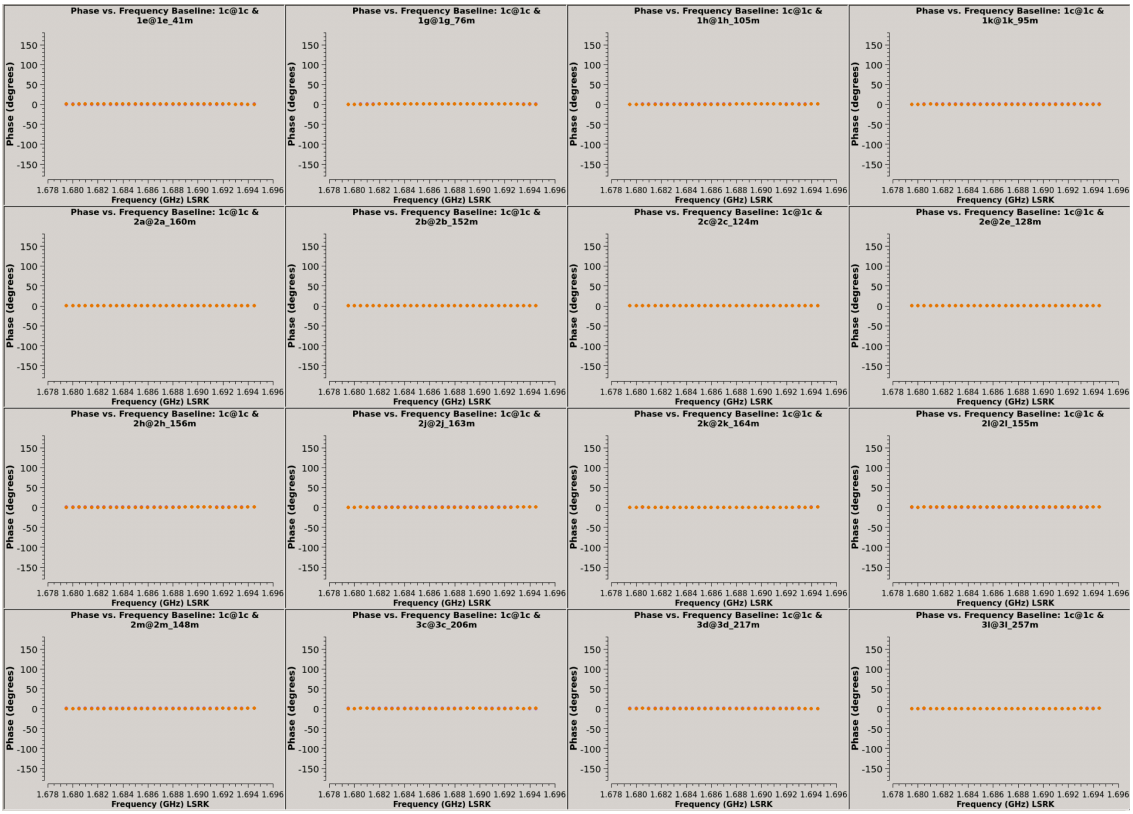

Figure 2: Same as Fig. 1, but after phase calibration. No residual phase is observed. Purple (X-polarization) data points are simply being obscured by the Orange (Y-polarization).

Fig. 2 shows the phase correctly solution applied on the data: flat phases, centered at 0 deg. The solution is then pushed on to the delay engine, which insures the antennas are phased up on the source.

2.2 Defining and measuring S/N

Fig. 3 shows the signal of interest overlaid on top of the bandpass amplitude response caused by the system's electronics. The bandpass shape for every antenna is different, making a signal-to-noise measurement non-trivial. To that, a 4th order polynomial fit of the noise floor, excluding the signal of interest, was performed, and subtracted from the data to correct for the bandpass effect. Fig. 3 shows the power spectrum density of an antenna, and the polynomial fit of the noise floor. Fig. 4 shows the normalized power spectral density after subtracting the noise baseline. No one-single-fit was enough to completely "flatten" the noise floor of all antennas, as can be seen in Fig. 4, but it was shown that this has no detrimental effects in the signal-to-noise measurement.

The signal-to-noise measurement that will be utilised throughout this memo is:

$$S/N = \mathrm{Peak}_{\mathrm{dB}} - \mathrm{Noise}_{\mathrm{dB}}, \tag{1}$$

where $\mathrm{Peak}_{\mathrm{dB}}$ is the mean power in dB measured measured in the 10 MHz signal

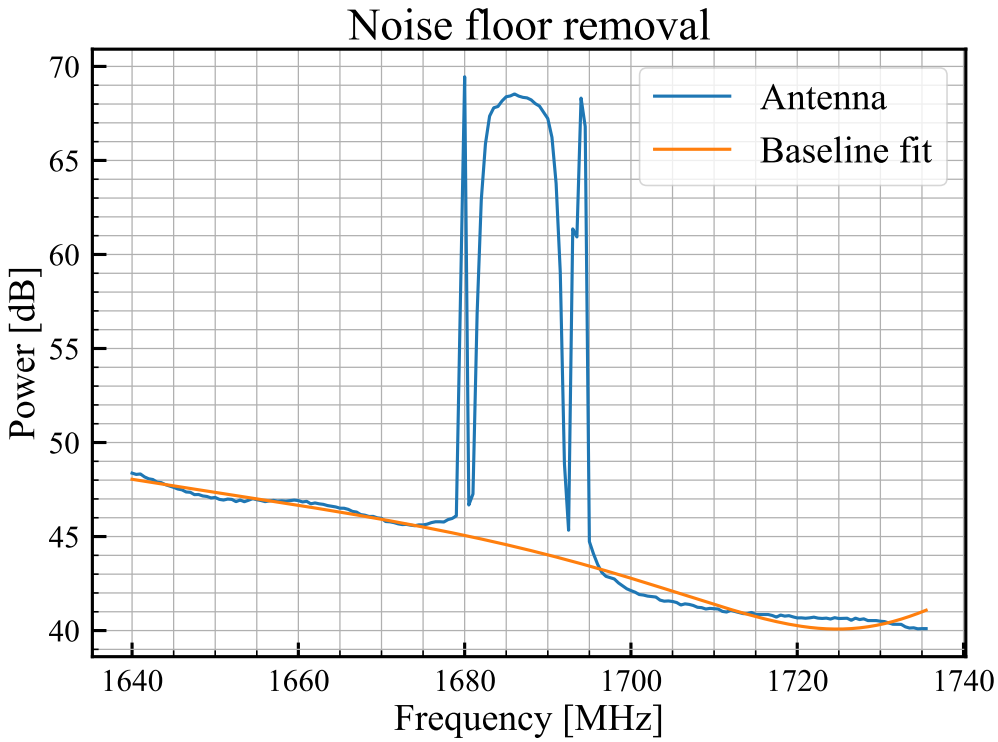

Figure 3: Power spectral density as a function of frequency for a single antenna. In orange, the polynomial fit to the baseline is shown.

band, and the Noise_{dB} is the mean power in dB of the noise floor. In practice, after the normalisation process described above, Noise_{dB} is assumed to be 0.

3 Results

Fig. 5 shows the S/N improvement as a function of the incremental addition of antennas to the coherent beamformer. The dashed line represents the ideal case scenario; in theory, the improvement in S/N should scale linearly with the number of the added antennas. As shown in the figure, the S/N improvement follows a strong linear dependence, showing that the behaviour of the beamformer is near-to-ideal. The fluctuations in S/N are due to the differences in sensitivities of the ATA feeds used in this experiment. No antenna weighting has been applied in this experiment, and all the antenna signals have been added in unison. For the interested reader, Tab. 1 lists the signal to noise ratio improvement with every added antenna.

4 Conclusion

This memo shows the efficiency of the ATA beamformer using the delay engine deployed on the RFSoC boards. Incremental increase in S/N, as a function of added

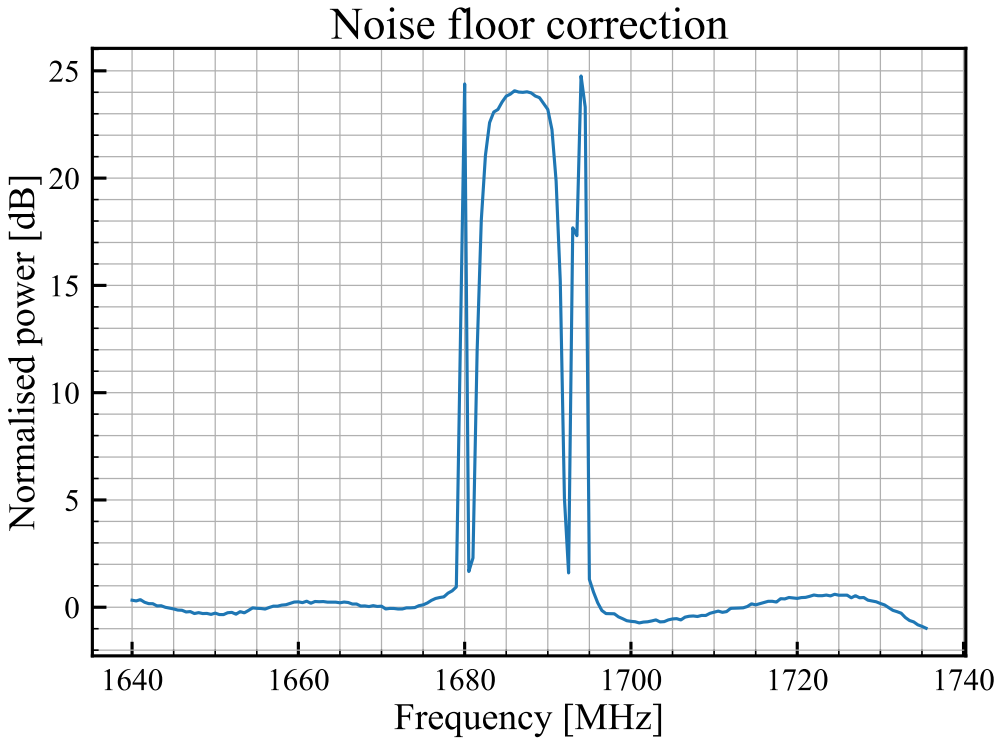

Figure 4: Normalised power of antenna shown in Fig. 3 after the removal of the noise baseline.

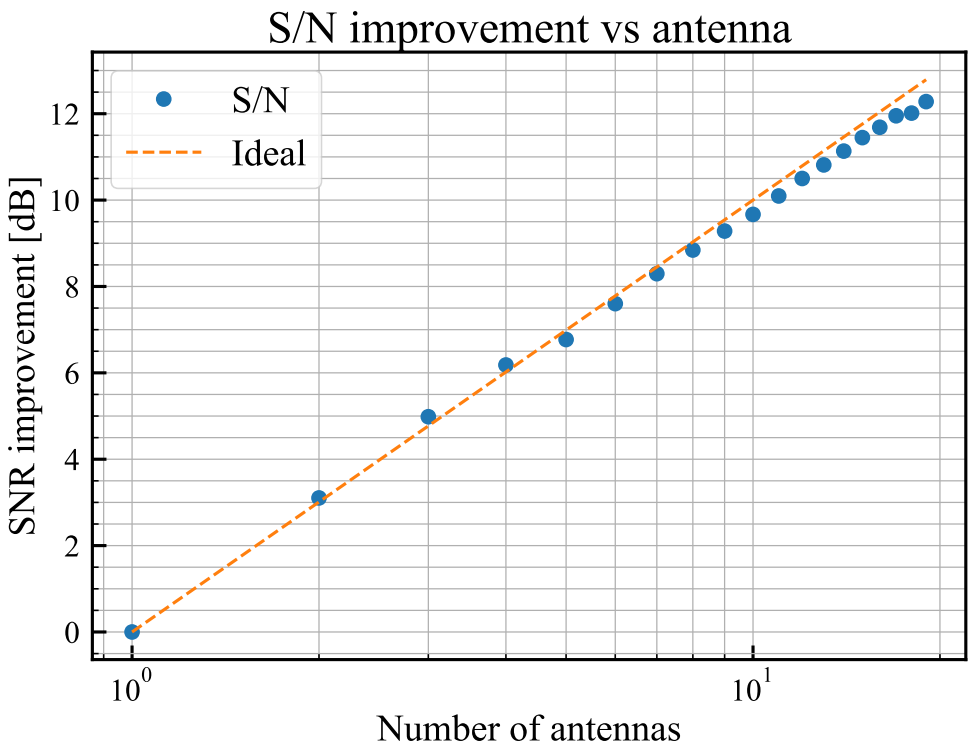

Figure 5: Signal to noise improvement as a function of added antennas to the coherent sum. Fluctuation of S/N around the ideal case scenario is caused by the difference in sensitivity of antennas.

Table 1: Signal to noise improvement with every added antenna to the coherent sum. The signal to noise value for every row represents the signal to noise of the sum of all the antennas listed above it.

Added antenna	S/N [dB]
2h	24.29
3l	27.40
3c	29.28
2c	30.47
5b	31.06
2l	31.90
1h	32.59
2b	33.14
1g	33.58
3d	33.96
4j	34.39
2a	34.79
1c	35.11
1k	35.43
2e	35.74
2j	35.98
2m	36.24
4g	36.31
2k	36.57

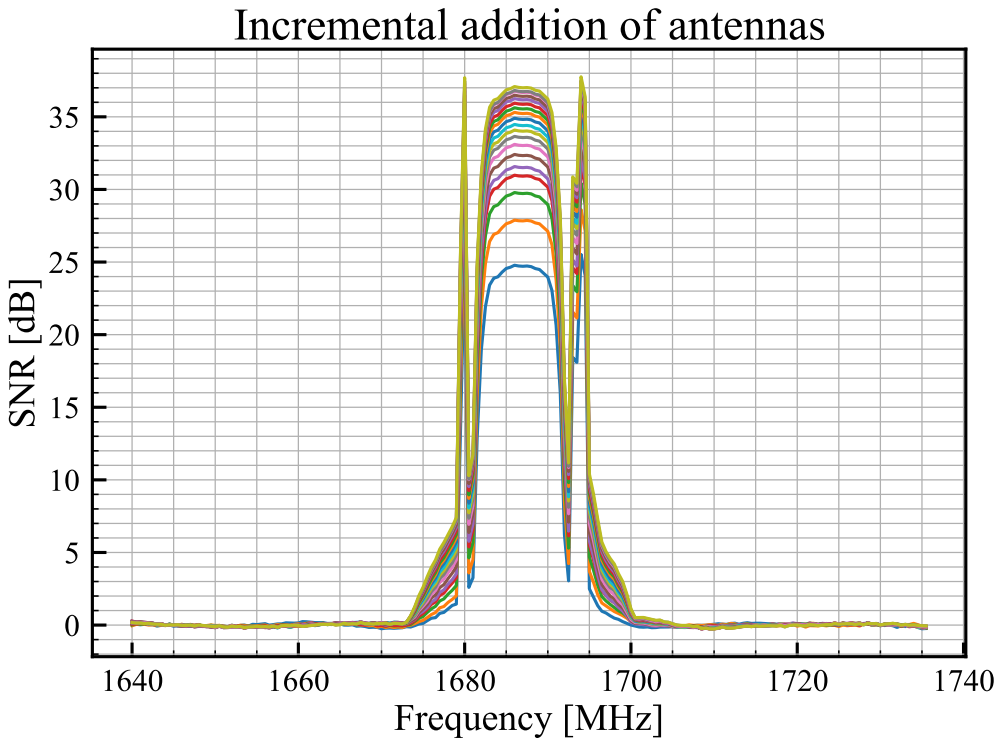

Figure 6: Spectra of the coherent sum with every added antenna, following Tab. 1.

antennas, was measured to be consistent with what is expected in an ideal case scenario. Improvements to the results might include weighting antenna signals by values proportional to their feeds' system temperature obtained using independent methods. A caveat that comes to mind is that for this particular observation, phase calibration and the beamformer observation were obtained on the same source, i.e. same position on the sky, which could hide many flaws including antenna position errors. A future experiment to validate and expand on this work would be to calibrate on one satellite, and observe another `GOES` satellite at a different position on the sky.